Revista Brasileira de Ciências Ambientais
Brazilian Journal of Environmental Sciences

Application of a convolutional neural network for automated multiclass identification of field-collected microplastics and diatom algae from optical microscopy images

Aplicação de uma rede neural convolucional para identificação automatizada multiclasse de microplásticos coletados em campo e algas diatomáceas utilizando imagens de microscopia óptica

Valéria de Almeida[1], *Giovana Katie Wiecheteck*[1], *Susete Wambier Christo*[1], *Pierre Girard*[2], *Jeanette Beber de Souza*[3], *João Eduardo Ferreira Inglez*[4], *Gabriel Staichak*[2], *Augusto Luiz Ferreira Júnior*[1]

ABSTRACT

Microplastics are present all around the globe, and they are a major threat to the environment because of the challenges they pose. Their sampling, isolation, and analysis processes are laborious and difficult due to their size, shape, and spreading dynamics. Furthermore, the lack of standardized protocols in microplastic research makes it difficult to compare results and unify the progress of the field. In this context, this work proposes and evaluates a model architecture based on deep learning to classify microplastic images using a dataset of real microplastics sampled from a freshwater reservoir, with convolutional neural network and transfer learning. Moreover, the model identifies diatom algae frustules, which can persist in the hydrogen peroxide degradation during the process of microplastic isolation due to their biosilica composition. The model was developed in Python using the Google Colab environment. A total of 1,140 images were used, and to ensure a robust and generalized evaluation, 5-fold cross-validation was applied. The model achieved 93% accuracy, with a recall of 97, 95, 92, and 90% for algae, microplastic filaments, fragments, and pellets, respectively. Overall, the accuracy of the model is encouraging considering the dataset size and all the challenges that involve the automatic identification of microplastics, with all their shape variations and nuances; thus the results are promising. To our knowledge, this is the first work addressing diatom presence after one of the most common microplastic isolation techniques and their automated classification among microplastics as well.

Keywords: deep learning; microalgae; freshwater; plastics.

RESUMO

Os microplásticos estão presentes em todo o mundo e são uma grande ameaça ao meio ambiente devido aos desafios que representam. Sua amostragem, isolamento e análise são processos trabalhosos e difíceis pelo seu tamanho, formato e dinâmica de propagação. Ademais, a falta de protocolos padronizados na pesquisa de microplásticos dificulta a comparação de resultados e a unificação do progresso na área. Neste contexto, este trabalho propõe e avalia uma arquitetura de modelo baseada em aprendizagem profunda para classificar imagens de microplásticos, com rede neural convolucional e aprendizagem por transferência, usando um conjunto de dados de microplásticos reais, amostrados de um reservatório de água doce. Além disso, o modelo identifica frústulas de algas diatomáceas, que podem persistir na degradação do peróxido de hidrogênio no processo de isolamento de microplásticos, devido à sua composição de biossílica. O modelo foi desenvolvido em Python pela plataforma do Google Colab. Foram utilizadas 1.140 imagens, e para garantir uma avaliação robusta e generalizada, foi aplicada a validação cruzada k-fold de 5 dobras. O modelo atingiu acurácia de 93%, com um *recall* de 97, 95, 92 e 90% para algas, filamentos microplásticos, fragmentos e pellets, respectivamente. A acurácia do modelo é encorajadora, considerando o tamanho do conjunto de dados e todos os desafios que envolvem a identificação automática de microplásticos, com suas variações de forma e nuances; então, os resultados são promissores. Conforme nosso conhecimento, este é o primeiro trabalho que aborda a presença de diatomáceas após uma das técnicas mais comuns de isolamento de microplásticos e, também, sua classificação automatizada entre microplásticos.

Palavras-chave: aprendizagem profunda; microalgas; água doce; plásticos.

[1]State University of Ponta Grossa – Ponta Grossa (PR), Brazil.

[2]Federal University of Mato Grosso – Cuiabá (MS), Brazil.

[3]State University of the Central West of Paraná – Irati (PR), Brazil.

Corresponding author: Valéria de Almeida. Avenida General Carlos Cavalcanti, 4.748, Bloco E – Campus Uvaranas – CEP: 84030-900 – Ponta Grossa (PR), Brazil. E-mail: vall_almeida_@hotmail.com

Conflicts of interest: the authors declare no conflicts of interest.

Funding: This work was supported by the Coordination for the Improvement of Higher Education Personnel (CAPES), Finance Code 001, and the Araucaria Foundation, agreement 211/2022.

Received on: 03/03/2025. Accepted on: 07/14/2025.

https://doi.org/10.5327/Z2176-94782491

Introduction

Microplastics are defined as polymeric particles up to 5 millimeters (He and Luo, 2020). They can be classified as primary, which are produced at microscopic dimensions, such as those found in hygiene products for exfoliation, or secondary, which are fragments of larger plastics that have deteriorated due to environmental factors (Costa and Duarte, 2022; Mathew et al., 2024). Assessing microplastics presents significant challenges due to their characteristics, sources, distribution dynamics, and persistence in the environment (Mitchell and Waterhouse, 2023). They can be transported via atmospheric deposition, percolation, surface runoff, and the release of effluents, as well as through the direct discharge of wastewater into rivers by both the population and industrial activities (Wang et al., 2022; Ivanic et al., 2023; Li, J. et al., 2023). Microplastics have been detected in both aquatic and terrestrial ecosystems, suspended in the air, present in rainwater, found in rural regions and even in polar areas (Citterich et al., 2023; Vithanage and Prasad, 2023).

Microplastics cause a noteworthy negative impact on organisms and the food web, by their ingestion and accumulation (Bostan et al., 2023; Li, X. et al., 2023). They can be transferred to other organisms, humans included through consumption, and carry toxic compounds such as pesticides, drugs, and metals (Tang et al., 2020; Benson et al., 2022). Microplastics in human bodies are a reality already, found even in the bloodstream and breast milk, and their presence could be linked to many health problems (Kutralam-Muniasamy et al., 2021; Ragusa et al., 2022; CalSPEC, 2023).

Microplastics are ubiquitous, and analyzing them is complicated by the lack of standardized methodologies and access to affordable, proper equipment (Kutralam-Muniasamy et al., 2021). Additionally, the analysis of microplastics tends to be labor-intensive and time-consuming (Lv et al., 2021). Many studies rely on human visual inspection using stereomicroscopy to examine particles, with only a small fraction undergoing further validation through techniques like Field Emission Gun with Energy Dispersive Spectroscopy (FEG-EDS), Raman, or Fourier Transform Infrared (FTIR) (Corcoran et al., 2019; Egessa et al., 2020; Gerolin et al., 2020; Nan et al., 2020; Lucas-Solis et al., 2021; Strady et al., 2021; Parvin et al., 2022; Drabinski et al., 2023; Kurki-Fox et al., 2023; Nayeri et al., 2023; Vidal et al., 2023; Castro et al., 2024; Duan et al., 2024; Saad et al., 2024).

Those studies usually classify microplastics according to their shape. This is relevant for understanding microplastic dynamics, how these particles are present in different environments, as well as their behavior, sources, properties, interactions, and implications within the environment. This could lead to future specific solutions applied to the reduction and removal of microplastics, enhancing their efficiency. However, the classification process, as it is, implies subjectivity and bias from various researchers worldwide (Hasnine et al., 2024). To solve this problem, this work aimed to present and evaluate the application of deep learning in the multiclass classification of microplastics through convolutional neural networks (CNNs).

In addition, this work provided the simultaneous identification of algae, specifically diatoms, since these were commonly encountered while handling the microplastics, making differentiation necessary. Diatoms are unicellular algae that have cell walls made of amorphous silica dioxide in two overlapping frustules, capable of remaining after organic matter degradation with hydrogen peroxide, a chemical treatment that is often used in microplastic isolation protocols (Barsanti and Gualtieri, 2023; Sun et al., 2024). Therefore, diatom frustules can remain after the microplastic isolation process and be found among them in the final samples.

Deep learning consists of an advanced machine learning technique in which the algorithm is capable of automatically learning patterns, rules, or mathematical relationships from the input data, in this case, images of microplastics, and using this knowledge to produce the desired output, namely identifying the microplastic class (Sharifani and Amini, 2013). In simpler terms, instead of programming the computer with specific instructions on how to recognize each type of microplastic, the algorithm learns to do so by analyzing a large number of examples.

The ResNet50 model is an example of this approach. It is a neural network architecture that has been previously trained on a vast collection of images (the ImageNet database), allowing it to recognize and classify new images by extracting and interpreting visual features, such as shapes, textures, and colors (Annable, 2024; MathWorks, 2024). This makes it a powerful tool for complex image classification tasks such as distinguishing between different types of microplastics.

Applying deep learning for the classification of microplastics presents significant challenges. First, a dataset of microplastic images is necessary, but currently, there is no available database. To accurately depict the true characteristics of microplastics as a pollution agent, it is essential to collect samples directly from the environment instead of generating artificial particles and images. The process involves collecting microplastics through media sampling, isolating and preparing the samples, and conducting thorough analyses. Afterward, images must be captured under suitable conditions and at an ideal resolution. These images must be properly sorted, treated, and in sufficient quantity to provide substantial input for the model.

The most challenging aspect is the heterogeneity of real microplastic shapes, even under the same class, when compared to artificially generated images or even microplastics obtained under controlled conditions (Giardino et al., 2023). For example, fibers could be large, thin, big, small, tangled, straight, bright colored, opaque, or transparent, similar to other classes, with many other singularities. While the human brain naturally recognizes complex visual patterns, achieving this through an automated algorithm presents a challenging task (Nielsen, 2024).

Many authors have addressed the automated processing of microplastics in recent years but the solutions often require expensive, specific equipment, products, or software. Giardino et al. (2023) proposed a semi-automatic image processing method for quantifying and measuring stained fluorescent microplastics using Nile Red dye. Lee et al. (2023) investigated the automatic identification of microplastics from

their Raman spectra, similar to Shi et al. (2022), through scanning electron micrographs, but also with classification.

Lorenzo-Navarro et al. (2021) developed an architecture to count and classify microplastics in images taken with a digital camera or mobile phone, at a resolution of at least 16 million pixels, without the need for microscopes, and only considering microplastics in the size range of 1 to 5 millimeters.

Since locations with significant pollution and sanitation problems are associated with higher microplastic concentrations, and consequently, environmental vulnerability (Strady et al., 2021), it is necessary to develop easily accessible, affordable, and effective solutions to facilitate the study of microplastics, especially in developing and underdeveloped countries. In this context, this work aimed to present and evaluate the application of deep learning in the multiclass classification of microplastics and algae through CNNs.

Methodology

Microplastic isolation

The microplastics used to train the model were isolated from sediment samples of Alagados Reservoir, which is responsible in part for the water supply of Ponta Grossa city. It is located in South Brazil, between coordinates 24°59' to 25°01' S and 49°58' to 50°03' W (Lemos et al., 2014). The samples were collected using a Ponar grab on six different occasions over 12 months. The sample processing was adapted from Laboratory Methods for the Analysis of Microplastics in the Marine Environment, by the National Oceanic and Atmospheric Administration Marine Debris Program (Masura et al., 2015), and consisted of density separation, sieving, organic matter digestion, and drying.

The microplastics were visually identified with an optic microscope at magnifications ranging from 40X to 400X, retrieving particles in the range of 0.075 to 5 millimeters, which were classified and photographed. The photos were taken with a smartphone Galaxy A22, at 2250 per 4000 pixels. A parcel of the microplastics was submitted to Scanning Electron Microscopy with Energy Dispersive Spectroscopy (SEM-EDS; TESCAN MIRA) for further investigation and validation (TESCAN Group, 2024).

Input images

A total of 3,459 particles were identified through visual inspection. Of these, 43.25% were classified as filaments, 34.58% as fibers, 10.38% as fragments, 7.31% as pellets, 2.49% as foams, and 1.99% as films. Although all particles were photographed, not all images were used as input for training the model due to issues with image quality or cluttered backgrounds. Additionally, the classes for foams and films lacked sufficient images to enable further classification. For pretreatment, the images were cropped to sizes ranging from 600 x 600 to 1,700 x 1,700 pixels. These images were then organized into folders, compressed into zip files, and uploaded to Google Drive.

A total of 953 fibers, 938 filaments, 300 fragments, 240 pellets, and 300 algae from the genus *Surirella* were manually selected and treated in this analysis. Other diatom genera, such as *Synedra, Pinnularia,* and *Aulacoseira*, were also observed during the microplastic analysis; however, since they had 60 or fewer photographs each, they were excluded from the analysis for insufficient input to train the model. To ensure that the number of images was equal across each class for the training process, the dataset was standardized to include 300 algae, 300 filaments, 300 fragments, and 240 pellets. Despite the large number of fiber images, this class was not used in the final code of this work because it is the most variable type of microplastic. Therefore, to train the model efficiently with the inclusion of this class, a larger dataset including the other classes is necessary, considering that the classes should preferably have a similar number of images to avoid bias. Since the current limiting number of images in the classes is 300, this alone would not be enough for efficient fiber differentiation. This resulted in a total of 1,140 images, with 912 allocated for training and 228 for validation. An ideal scenario would involve increasing the dataset size to further enhance the training and precision of the model. Figure 1 illustrates the microplastics and algae.

Model

The algorithm was coded in Python version 3.10.12 via Google Colab, using TensorFlow version 2.18.0 with Keras API. The architecture was based on the books by Chollet (2018), Gosh and Math (2023), Zhang et al. (2023) and Ansari (2024), with the structure and debugging assistance of artificial intelligence tools. The code was structured to use TensorFlow's deep learning to train the identification of microplastics in classes with a dataset of classified images of real microplastics, using the Resnet50 architecture of CNN and transfer learning to classify new images. The code was executed in a Dell Inspiron 15 5000, core i5, with 4 gigabytes of RAM.

The ResNet50 was chosen for this study due to its proven effectiveness in image classification involving complex and subtle features, which is essential while distinguishing between different types of microplastics and algae. Although lighter architectures such as MobileNet, EfficientNet, and SqueezeNet offer faster inference and lower computational cost, they would not meet the depth and feature extraction capability required in this study. The residual learning framework of ResNet50 allows maintaining high accuracy even in deep configurations, mitigating the vanishing gradient problem and enabling it to learn intricate patterns from small datasets through transfer learning.

This model has also been widely adopted in similar scientific applications involving biomedical imaging, microscopic particle identification, and environmental monitoring due to its balance between performance and generalizability. Given the complexity of our classes and the limited availability of high-quality field-collected training data, ResNet50 was the most suitable choice to ensure robustness without the need for extensive hyperparameter tuning or computational infrastructure beyond the available resources.

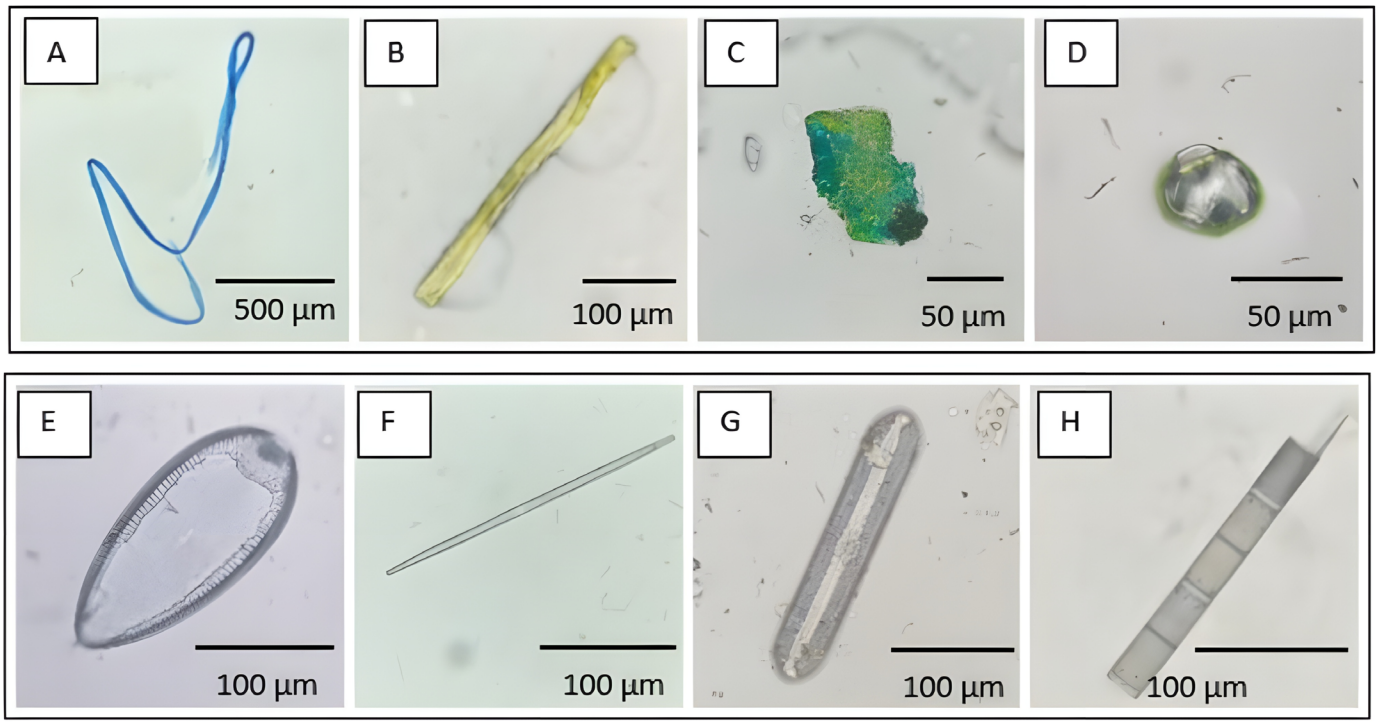

Figure 1 – Microplastics and algae observed in the samples: (A) Fiber; (B) Filament; (C) Fragment; (D) Pellet; (E) *Surirella* sp.; (F) *Synedra* sp.; (G) *Pinnularia* sp., and (H) *Aulacoseira* sp.

The process of coding optimization involves multiple iterations of architecture and input modifications. The final model architecture begins with the installation of TensorFlow and the importation of the necessary libraries. It then proceeds to extract the microplastic images stored in a zip file on Google Drive, creating a directory for the extracted folder. The microplastic shapes can vary in color, primarily being transparent or displaying faded hues. After testing and consideration, the next step in the code was to convert the images to grayscale. This transformation ensures that the classification focuses on the shape of the particles rather than associating specific colors with particular shapes.

Data augmentation techniques were employed to enhance the ability of the model to generalize and reduce overfitting, especially considering the limited dataset available. Specifically, during training, images were subjected to a set of controlled transformations using the ImageDataGenerator function in TensorFlow. These transformations included random rotations of up to 30 degrees, horizontal flips, zoom variations up to 20%, and translations (shifts) of up to 10% in both horizontal and vertical directions. Additionally, the nearest fill mode was applied across all training folds for experimental reproducibility and to allow the model to better learn the invariant features of the microplastic images.

The images were resized to 256 by 256 pixels, which is a standard size for CNN analysis. This size strikes a balance between higher detail compared to smaller sizes and better computational efficiency than larger sizes. Larger dimensions, such as 526 or 1,024 pixels, would offer more detail, but the available equipment could not support them. The dataset was split into 80% for training and 20% for validation, with class weights set inversely proportional to the number of images in each class.

Since ResNet50 is a pre-trained model, fine-tuning was achieved by unfreezing the first 100 layers for training. The output layer corresponds to the classes of microplastics and algae. The model was then compiled using the Adam optimizer to adjust the weights during deep learning. To prevent overfitting—where the model performs well on the training dataset but fails to generalize to new data—an early stopping function was implemented with a patience of 10 epochs. The accuracy and loss for each epoch were printed during training for monitoring purposes. After the conclusion of the training, the details about the process, precision, recall, F1-score, and confusion matrix were shown.

In this work, a default set of hyperparameters was employed, such as a learning rate of $1e^{-4}$, batch size of 32, and 50 training epochs, in combination with callbacks for early stopping and adaptive learning rate reduction. No formal hyperparameter optimization (such as grid search, random search, or Bayesian optimization) was conducted. This decision was made due to computational resource limitations and the extended runtime required by k-fold cross-validation using a ResNet50 architecture. Instead, hyperparameters were selected based on values commonly reported in similar image classification tasks in the

literature. This choice is acknowledged here to maintain methodological transparency and provide context for the reported performance.

Results and Discussion

The execution of the code resulted in five models; each trained with different sets of images. The best model, result of the first fold, had 33 batches of 29 images per epoch, taking an average of 18 seconds per step, and approximately 492 to 566 seconds per epoch. The training was halted at epoch 33 of 50 due to early stopping, which was triggered by a patience of 10. This means that after epoch 33, the validation accuracy stopped improving, and the model was not generalizing any better, despite the increase in training accuracy.

The training and validation accuracy and loss are illustrated in Figure 2. The training accuracy showed an increase throughout the process, rising at a higher rate during the first 5 epochs, as expected. In the first epochs, the model is most likely adjusting the weights while learning basic features. As training progresses, it begins to learn more refined and complex features, which slows down the pace of improvement after the initial epochs. It began at 35% in the first epoch and reached 93% by epoch 33.

The validation accuracy started at 19% and greatly improved, reaching 87% at epoch 13 after consistently increasing. It was also expected, as the model was beginning to adjust its parameters, learning to generalize well to the validation set. However, it experienced a fluctuation, dropping to 68% in epoch 16, before finishing at 93% in epoch 33.

The loss metrics during training and validation shows a decline in both cases over the epochs, indicating that the model is learning and that the predictions are increasingly close to the ground truth. The training loss decreased steadily, from 1.4 to 0.2, while the validation loss exhibited a spike at epoch 5 before a more gradual decline throughout the epochs, from 1.6 to 7.5, then 0.2.

The best model report, presented in Table 1, outlines the prediction results derived from the validation dataset. Among the various types of microplastics assessed, pellets were identified with the highest precision at 98%, followed by fragments at 92%, and filaments at 89%. Notably, the model achieved a precision rate of 97% in identifying the algae class, likely due to the consistent shape of algae compared to the diverse shapes observed in microplastics, even within the same classification. This variability underscores the necessity for larger datasets to enhance the model's training. By expanding the dataset, it is possible to improve pattern recognition and produce more accurate predictions.

In contrast, filaments showed the highest recall among the microplastics with a rate of 95%. This was followed by fragments at 92% and pellets at 90%. Algae also had a high recall value of 97%. The difference between the precision and recall for the filament category indicates that the model is generating more false positives and fewer false negatives, accurately predicting real positives at a 95% rate.

Table 1 – Graphical representation of the training and validation accuracy of the first fold.

	Precision	Recall	F1 score	Support
Filament	0.89	0.95	0.92	60
Fragment	0.92	0.92	0.92	60
Pellet	0.98	0.90	0.93	48
Algae	0.97	0.97	0.97	60
Macro average	0.94	0.93	0.93	228
Weighted average	0.94	0.93	0.93	228
Accuracy			0.93	228

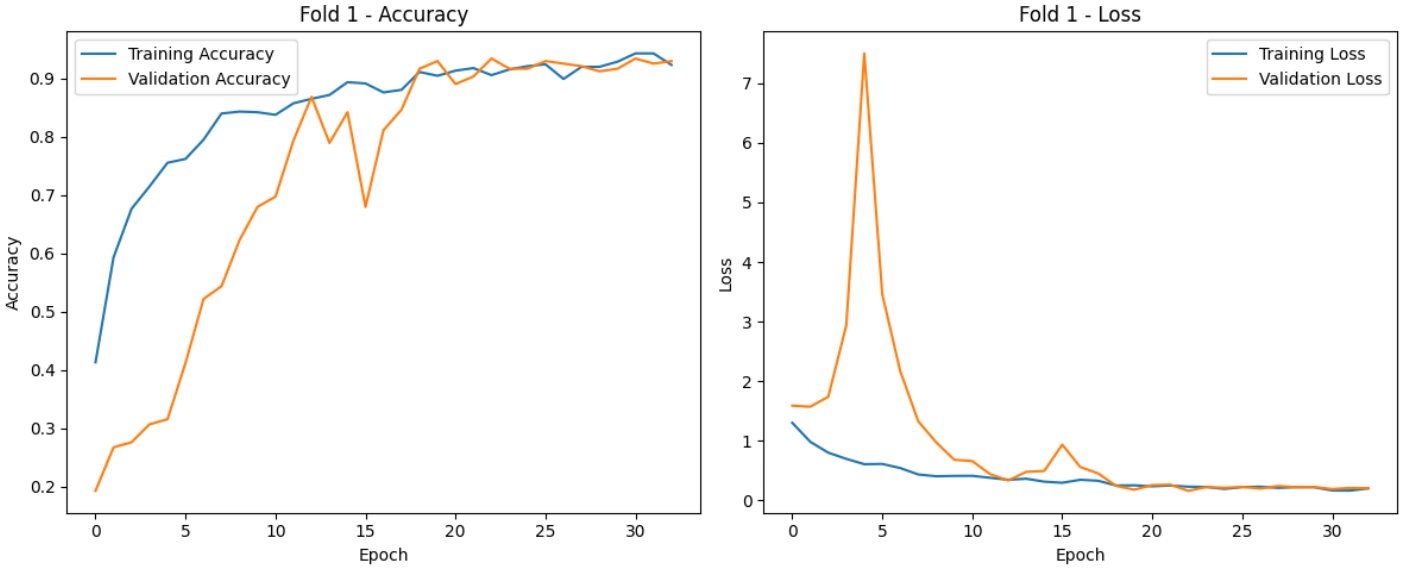

Figure 2 – Graphical representation of the training and validation accuracy and loss.

Conversely, for the pellet class, the model tends to generate more false negatives than false positives. This discrepancy is reflected in the F1 score, which is the harmonic mean of precision and recall. The support refers to the size of the validation sample, while accuracy is the mean of the F1 score. An accuracy value of 93% is satisfactory given the dataset size; however, there is still a need for improvement with a larger training input.

The confusion matrix (Figure 3) illustrates the actual values, false negatives, and false positives of the predictions. The algae class had the highest number of true positive predictions, followed by filaments, fragments, and pellets. The errors basically involved misidentifying actual fragments as filaments (3 instances) and actual pellets as filaments (3 instances). This suggests that the model tends to over-predict filaments and struggles with accurately classifying pellets, resulting in false positives and false negatives for this category. These issues also impacted the precision and recall of the fragments.

The results of the other folds are shown in Table 2. Folds 2, 4, 5, and 6 showed similar results to fold 1, while fold 3 showed notably unsatisfactory results. The 0% F1 score achieved by three of the four categories indicates a probable bad set of training images, which precluded the model from properly learning the features of the images of different classes. The 100% recall of pellets suggests a bias from the model towards this class to the detriment of the others.

The results obtained across different folds of the cross-validation process reveal variations in model performance across the validation subsets, both in terms of accuracy and class discrimination capability, as shown in Figure 4. Although the training accuracy showed a similar tendency across all folds, rapidly increasing at the first epochs and then maintaining slow improvements, the validation accuracy showed considerable variations. In fold 2, the validation accuracy took some epochs to start improving, then spiked at epoch 14. Folds 4 and 5 showed a more gradual improvement, meanwhile fold 3 barely showed improvement in its validation accuracy.

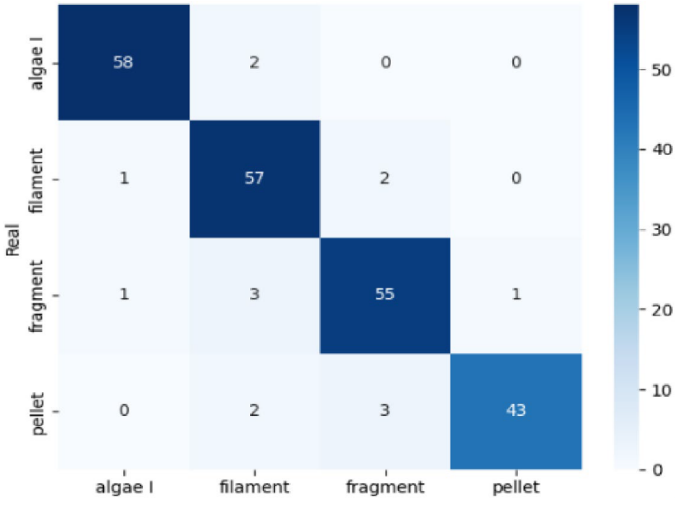

Figure 3 – Confusion matrix of the validation dataset.

While all losses tended to decrease, fold 3 showed an increasing validation loss, indicating its distancing from the ground truth.

The overall evaluation of the model across the five cross-validation folds yielded an average validation accuracy of 77.40%, standard deviation ±28.30%, and an average F1 score of 74.60±33.89%. These results reflect generally strong performance but also suggest a considerable degree of variability across the folds.

Looking at the per-fold results, the model demonstrated excellent performance in folds 1, 2, 4, and 5, with both validation accuracies and F1 scores ranging from 89 to 96,%, as shown in Figure 5. This indicates that, in these cases, the model was highly effective at correctly classifying the target classes and maintaining a strong balance between precision and recall.

Table 2 – Graphical representation of the training and validation accuracy of folds 2 to 5.

		Precision	Recall	F1 score	Support
Fold 2	Filament	0.95	0.93	0.94	60
	Fragment	0.88	0.85	0.86	60
	Pellet	0.88	0.96	0.92	48
	Algae	0.97	0.95	0.96	60
	Macro average	0.92	0.92	0.92	228
	Weighted average	0.92	0.92	0.92	228
	Accuracy			0.92	228
Fold 3	Filament	0.00	0.00	0.00	60
	Fragment	0.00	0.00	0.00	60
	Pellet	0.21	1.00	0.35	48
	Algae	0.00	0.00	0.00	60
	Macro average	0.05	0.25	0.09	228
	Weighted average	0.04	0.21	0.07	228
	Accuracy			0.21	228
Fold 4	Filament	0.94	0.98	0.96	60
	Fragment	0.87	0.78	0.82	60
	Pellet	0.91	0.88	0.89	48
	Algae	0.92	1.00	0.96	60
	Macro average	0.91	0.91	0.91	228
	Weighted average	0.91	0.91	0.91	228
	Accuracy			0.91	228
Fold 5	Filament	0.88	0.97	0.92	60
	Fragment	0.88	0.77	0.82	60
	Pellet	0.86	0.88	0.87	48
	Algae	0.95	0.97	0.96	60
	Macro average	0.89	0.89	0.89	228
	Weighted average	0.89	0.89	0.89	228
	Accuracy			0.89	228

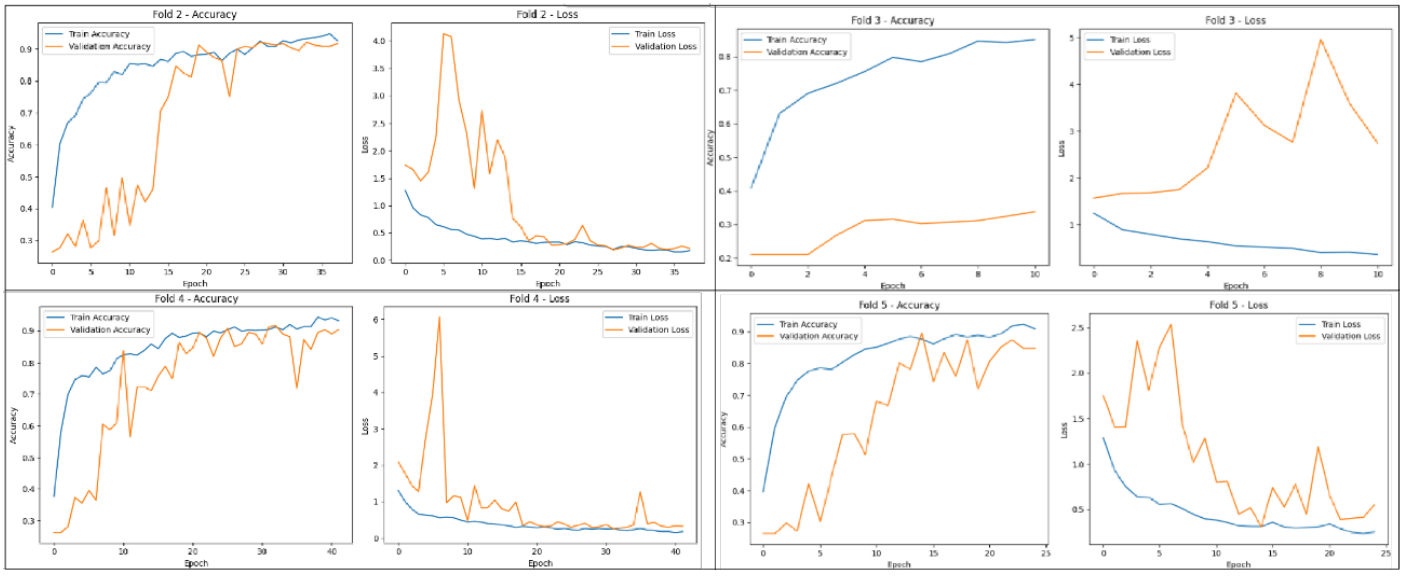

Figure 4 – Graphical representation of the training and validation accuracy and loss in different folds of the cross-validation (fold 2 at top left, fold 3 at top right, fold 4 at bottom left, and fold 5 at bottom right).

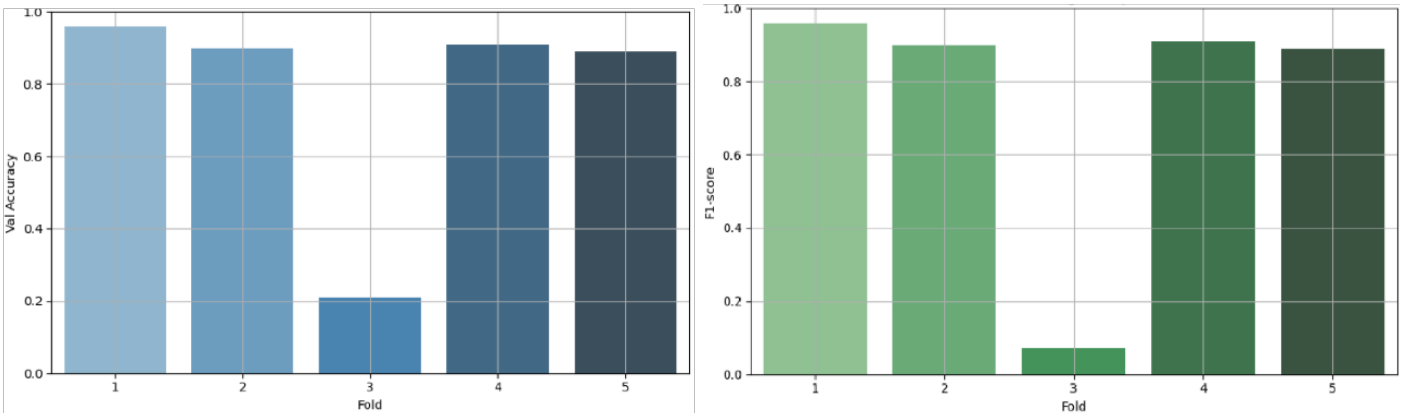

Figure 5 – Validation accuracy per fold.

Fold 3, in turn, stands out as a significant outlier, with a validation accuracy of only 21% and an F1 score of 7%. This sharp decline in performance suggests that the data in fold 3 may have presented unique challenges to the model, potentially due to class imbalance, noisy data, or a distribution that differs markedly from the training set in that iteration. The relatively high standard deviations observed for both accuracy and F1 score further confirm the presence of this performance inconsistency, largely driven by the poor outcome in fold 3.

In summary, while the model exhibits strong and reliable performance in most folds, the substantial drop in fold 3 highlights the importance of increasing the size of the dataset to improve the training and validation process, providing a more resourceful distribution across all folds.

After conducting training and validation, the model based on fold 1 was prepared to predict new images, displaying their filenames and predicted classes. The architecture of the model was designed to classify each image from a specific folder, returning results in the format: "Prediction for the image ({image_path}): {predicted_class}". Each prediction was completed in less than a second. The model achieved an accuracy of 95% when tested with 40 new real images of algae and microplastics.

Conclusion

This study is the first to address the presence of diatom frustules following the most common microplastic isolation protocol, which involves degrading organic matter using hydrogen peroxide. Additionally, it introduces an automatic classification system that categorizes microplastics and algae into four distinct groups. The final model's

overall accuracy was 93%, and its precision in recognizing algae was 97%. These results are promising, especially considering the size of the dataset and the challenges associated with the automatic identification of microplastics, which come in various shapes. Future research should expand the dataset to include over 1,000 images per class, with more microplastic classes and incorporate additional diatom species into the classification, as these can resemble microplastic filaments. Accurate identification of these algae is essential.

Data Availability

The data that support the findings of this study are openly available in Mendeley Data at http://doi.org/10.17632/yyn2g83vsy.1

Acknowledgements

The authors would like to thank the Water and Sanitation Company of Parana (Sanepar) and the State University of Ponta Grossa for all the assistance received during the processing of the analysis.

Authors' Contributions

Almeida, V.: Conceptualization, Methodology, Software, Formal Analysis, Investigation, Data Curation, Writing – Original Draft, Visualization. **Wiecheteck**, G.K.: Conceptualization, Resources, Writing – Review & Editing, Supervision, Funding Acquisition. **Christo**, S.W.: Conceptualization, Resources, Writing – Review & Editing, Project Administration. **Girard**, P.: Writing – Review & Editing. **Souza**, J.B.: Writing – Review & Editing. **Inglez**, J.E.F.: Conceptualization, Resources, Formal Analysis, Writing – Review & Editing, Visualization. **Staichak**, G.: Conceptualization, Methodology, Formal Analysis. **Ferreira Júnior**, A.L.: Formal Analysis, Investigation, Project Administration.

References

Annable, C., 2024. Python machine learning: a step-by-step journey with scikit-learn and tensor flow for beginners.

Ansari, H., 2024. Mastering tensorflow: unleashing the power of deep learning: a hands-on guide to building neural networks, image processing, and natural language understanding with tensorflow (Accessed August 14, 2025) at:. https://sciarium.com/file/632232/

Barsanti, L.; Gualtieri, P., 2023. Algae: anatomy, biochemistry, and biotechnology, Third edition. CRC Press, Boca Raton. https://doi.org/10.1201/9781003187707

Benson, N.U.; Agboola, O.D.; Fred-Ahmadu, O.H.; De-La-Torre, G.E.; Oluwalana, A.; Williams, A.B., 2022. Micro(nano)plastics prevalence, food web interactions, and toxicity assessment in aquatic organisms: a review. Frontiers in Marine Science, v. 9, 851281. https://doi.org/10.3389/fmars.2022.851281

Bostan, N.; Ilyas, N.; Akhtar, N.; Mehmood, S.; Saman, R.U.; Sayyed, R.Z.; Shatid, A.A.; Alfaifi, M.Y.; Elbehairi, S.E.I.; Pandiaraj, S., 2023. Toxicity assessment of microplastic (MPs). Environmental Research, v. 234, 116523. https://doi.org/10.1016/j.envres.2023.116523

California State Policy Evidence Consortium (CalSPEC), 2023. Microplastics occurrence, health effects, and mitigation policies: an evidence review for the California state legislature. CalSPEC, United States of America.

Castro, D.G.D.; Silva, A.L.L.D.; Lopes, M.D.N.; Freire, A.S.; Leite, N.K., 2024. Effect of urbanization and water quality on microplastic distribution in Conceição Lagoon watershed, Brazil. Environmental Science and Pollution Research, 31, 28870-28889. https://doi.org/10.1007/s11356-024-33029-y

Chollet, F., 2018. Deep learning with python. Manning Publications Co., Shelter Island.

Citterich, F.; Giudice, A.L.; Azzaro, M., 2023. A plastic world: A review of microplastic pollution in the freshwaters of the Earth's poles. Science of The Total Environment, v. 869, 161847. https://doi.org/10.1016/j.scitotenv.2023.161847

Corcoran, P.L.; Belontz, S.L.; Ryan, K.; Walzak, M.J., 2019. Factors controlling the distribution of microplastic particles in benthic sediment of the Thames River, Canada. Environmental Science & Technology, v. 54 (2), 818-825. https://doi.org/10.1021/acs.est.9b04896

Costa, J.P.; Duarte, A.C., 2022. Introduction to the analytical methodologies for the analysis of microplastics. In: Rocha-Santos, T.AP., Costa, M.F.; Mouneyrac, C. (Eds.), Handbook of microplastics in the environment. Springer, Cham. https://doi.org/10.1007/978-3-030-39041-9_1

Drabinski, T.L.; Carvalho, D.G.D.; Gaylarde, C.C.; Lourenço, M.F.P.; Machado, W.T.V.; Fonseca, E.M.; Silva, A.L.C.D.; Baptista Neto, J.A., 2023. Microplastics in freshwater river in Rio de Janeiro and its role as a source of microplastic pollution in Guanabara Bay, SE Brazil. Micro, v. 3 (1), 208-223. https://doi.org/10.3390/micro3010015

Duan, L.; Luo, L.; Zhang, L.; Li, D.; Li, H.; Xu, T.; Xu, J.; Zhang, H., 2024. The occurrence of microplastics pollution in the surface water and sediment of Lake Chenghai in Southwestern China. Water, v. 16 (18), 2672. https://doi.org/10.3390/w16182672

Egessa, R.; Nankabirwa, A.; Ocaya, H.; Pabire, W.G., 2020. Microplastic pollution in surface water of Lake Victoria. Science of the Total Environment, v. 741, 140201. https://doi.org/10.1016/j.scitotenv.2020.140201

Gerolin, C.R.; Pupim, F.N.; Sawakuchi, A.O.; Grohmann, C.H.; Labuto, G.; Semensatto, D., 2020. Microplastics in sediments from Amazon rivers, Brazil. Science of the Total Environment, v. 749, 141604. https://doi.org/10.1016/j.scitotenv.2020.141604

Giardino, M.; Balestra, V.; Janner, D.; Bellopede, R., 2023. Automated method for routine microplastic detection and quantification. Science of The Total Environment, vol. 859 (Part 2), 160036. https://doi.org/10.1016/j.scitotenv.2022.160036

Gosh, T.; Math, S.K.B., 2023. Practical mathematics for AI and deep learning. BPB Publications, India.

Hasnine, M.D.T.; Anik, A.H.; Alam, M.; Yuan, Q., 2024. Navigating microplastic challenges: separation and detection strategies in wastewater treatment. In: Kumar, A.; Singh, V. (Eds.), Microplastics pollution and its remediation. Springer, Cham.

He, D.; Luo, Y., 2020. Microplastics in terrestrial environments emerging contaminants and major challenges. In: Barceló, D.; Kostianoy, A.G. (Eds.), The handbook of environmental chemistry (Vol. 95). Springer, Cham. https://doi.org/10.1007/978-3-030-56271-7

Ivanic, F.M.; Guggenberger, G.; Woche, S.K.; Bachmann, J.; Hoppe, M.; Carstens, J.F., 2023. Soil organic matter facilitates the transport of microplastic by reducing surface hydrophobicity. Colloids and Surfaces A: Physicochemical and Engineering Aspects, v. 676 (Part B), 132255. https://doi.org/10.1016/j.colsurfa.2023.132255

Kurki-Fox, J.J.; Doll, B.A.; Monteleone, B.; West, K.; Putnam, G.; Kelleher, L.; Krause, S.; Schneidewind, U., 2023. Microplastic distribution and characteristics across a large river basin: Insights from the Neuse River in North Carolina, USA. Science of the Total Environment, 878, 162940. https://doi.org/10.1016/j.scitotenv.2023.162940

Kutralam-Muniasamy, G.; Pérez-Guevara, F.; Elizalde-Martínez, I.; Shruti, V.C., 2021. How well-protected are protected areas from anthropogenic microplastic contamination? Trends in Environmental Analytical Chemistry, (32), e00147. https://doi.org/10.1016/j.teac.2021.e00147

Lee, S.; Jeong, H.; Hong, S.M.; Yun, D.; Lee, J.; Kim, E.; Cho, K.H., 2023. Automatic classification of microplastics and natural organic matter mixtures using a deep learning model. Water Research, v. 246, 120710. https://doi.org/10.1016/j.watres.2023.120710

Lemos, C.F.; Fiori, A.P.; Oka-Fiori, C.; Tomazoni, J.C., 2014. Assoreamento da represa de Alagados pela contribuição de sedimentos da bacia hidrográfica do alto curso do rio Pitangui/PR. Geociências, v. 33 (4), 549-557 (Accessed August 14, 2025) at:. https://www.periodicos.rc.biblioteca.unesp.br/index.php/geociencias/article/view/9501

Li, J.; Zhang, J.; Ren, S.; Huang, D.; Liu, F.; Li, Z; Zhang, H.; Zhao, M.; Cao, Y.; Mofolo, S.; Liang, J.; Xu, W.; Jones, D.L.; Chadwick, D.R.; Liu, X.; Wang, K., 2023. Atmospheric deposition of microplastics in a rural region of North China Plain. Science of the Total Environment, v. 877, 162947. https://doi.org/10.1016/j.scitotenv.2023.162947

Li, X.; Bao, L.; Wei, Y.; Zhao, W.; Wang, F.; Liu, X.; Su, H.; Zhang, R., 2023. Occurrence, bioaccumulation, and risk assessment of microplastics in the aquatic environment: a review. Water, 15 (9), 1768. https://doi.org/10.3390/w15091768

Lorenzo-Navarro, J.; Castrillón-Santana, M.; Sánchez-Nielsen, E.; Zarco, B.; Herrera, A.; Martínez, I.; Gómez, M., 2021. Deep learning approach for automatic microplastics counting and classification. Science of the Total Environment, v. 765, 142728. https://doi.org/10.1016/j.scitotenv.2020.142728

Lucas-Solis, O.; Moulatlet, G.M.; Guamangallo, J.; Yacelga, N.; Villegas, L.; Galarza, E.; Rosero, B.; Zurita, B.; Sabando, L.; Cabrera, M.; Gimiliani, G.T.; Capparelli, M.V., 2021. Preliminary assessment of plastic litter and microplastic contamination in freshwater depositional areas: The case study of Puerto Misahualli, Ecuadorian Amazonia. Bulletin of Environmental Contamination and Toxicology, v. 107, 45-51. https://doi.org/10.1007/s00128-021-03138-2

Lv, L.; Yan, X.; Feng, L.; Jiang, S.; Lu, Z.; Xie, H.; Sun, S.; Chen, J.; Li, C., 2021. Challenge for the detection of microplastics in the environment. Water Environment Research, v. 93 (1), 5-15. https://doi.org/10.1002/wer.1281

Masura, J.; Baker, J.; Foster, G.; Arthur, C.; Herring, C., 2015. Laboratory methods for the analysis of microplastics in the marine environment. Silver Spring, United States (Accessed August 14, 2025) at:. https://repository.library.noaa.gov/view/noaa/10296

Mathew, J.T.; Inobeme, A.; Adetuyi, B.O.; Falana, Y.O.; Adetunji, C.O.; Shahnawaz, M., 2024. Application of microplastics in toiletry products. In: Shahnawaz, M.; Adetunji, C.O.; Dar, M.A.; Zhu, D. (Eds.), Microplastic pollution. Springer, Singapore. https://doi.org/10.1007/978-981-99-8357-5_5

Mathworks. Resnet50. Website (Accessed November 15, 2024) at:. https://www.mathworks.com/help/de eplearning/ref/resnet50.html

Mitchell, C.; Waterhouse, J., 2023. Microplastics in Arctic Sea ice: a petromodern archive fever. In: Konrad, T. (Ed.), Plastics, environment, culture, and the politics of waste. Edinburgh University Press, Edinburgh. https://doi.org/10.3366/edinburgh/9781399511735.003.0006

Nan, B.; Su, L.; Kellar, C.; Craig, N.J.; Keough, M.J.; Pettigrove, V., 2020. Identification of microplastics in surface water and Australian freshwater shrimp Paratya australiensis in Victoria, Australia. Environmental Pollution, v. 259, 113865. https://doi.org/10.1016/j.envpol.2019.113865

Nayeri, D.; Mousavi, S. A.; Almasi, A.; Asadi, A., 2023. Microplastic abundance, distribution, and characterization in freshwater sediments in Iran: a case study in Kermanshah city. Environmental Science and Pollution Research, v. 30 (17), 49817-49828. https://doi.org/10.1007/s11356-023-25620-6

Nielsen, M. Neural networks and deep learning (Accessed November 11, 2024) at:. http://neuralnetworksanddeeplearning.com/index.html

Parvin, F.; Hassan, A.; Tareq, S.M., 2022. Risk assessment of microplastic pollution in urban lakes and peripheral Rivers of Dhaka, Bangladesh. Journal of Hazardous Materials Advances, v. 8, 100187. https://doi.org/10.1016/j.hazadv.2022.100187

Ragusa, A.; Notarstefano, V.; Svelato, A.; Belloni, A.; Gioacchini, G.; Blondeel, C.; Zucchelli, E.; De Luca, C.; D'Avino, S.; Gulotta, A.; Carnevali, O.; Giorgini, E., 2022. Raman microspectroscopy detection and characterisation of microplastics in human breastmilk. Polymers, v. 14 (13), 2700. https://doi.org/10.3390/polym14132700

Saad, D.; Ramaremisa, G.; Ndlovu, M.; Chauke, P.; Nikiema, J.; Chimuka, L., 2024. Microplastic abundance and sources in surface water samples of the Vaal River, South Africa. Bulletin of Environmental Contamination and Toxicology, v. 112 (1), 23. https://doi.org/10.1007/s00128-023-03845-y

Sharifani, K.; Amini, M., 2013. Machine learning and deep learning: a review of methods and applications. World Information Technology and Engineering Journal, v. 10 (7), 3897-3904 (Accessed August 14, 2025) at:. https://ssrn.com/abstract=4458723

Shi, B.; Patel, M.; Yu, D.; Yan, J.; Li, Z.; Petriw, D.; Pruyn, T.; Smyth, K.; Passeport, E.; Miller, R.J.D.; Howe, J.Y., 2022. Automatic quantification and classification of microplastics in scanning electron micrographs via deep learning. Science of the Total Environment, v. 825, 153903. https://doi.org/10.1016/j.scitotenv.2022.153903

Strady, E.; Dang, T.H.; Dao, T.D.; Dinh, H.N.; Do, T.T.D.; Duong, T.N.; Duong, T.T.; Hoang, D.A.; Kieu-Le, T.C.; Le, T.P.Q.; Mai, H.; Trinh, D.M.; Nguyen, Q.H; Tran-Nguyen, Q.A.; Tran, Q.V.; Truong, T.N.S.; Chu, V.H.; Vo, V.C., 2021. Baseline assessment of microplastic concentrations in marine and freshwater environments of a developing Southeast Asian country, Viet Nam. Marine Pollution Bulletin, v. 162, 111870. https://doi.org/10.1016/j.marpolbul.2020.111870

Sun, X.; Zhang, M.; Liu, J.; Hui, G.; Chen, X.; Feng, C., 2024. The art of exploring diatom biosilica biomaterials: from biofabrication perspective. Advanced Science, v. 11 (6), 2304695. https://doi.org/10.1002/advs.202304695

Tang, Y.; Liu, Y.; Chen, Y.; Zhang, W.; Zhao, J.; He, S.; Yang, C.; Zhang, T.; Tang, C.; Zhang, C.; Yang, Z., 2020. A review: Research progress on microplastic pollutants in aquatic environments. Science of the Total Environment, v. 766, 142572. https://doi.org/10.1016/j.scitotenv.2020.142572

TESCAN Group. TESCAN MIRA (Accessed September 13, 2024) at:. https://www.tescan.com/pt-br/product/sem-for-materials-science-tescan-mira/

Vidal, A.; Phuong, N.N.; Métais, I.; Gasperi, J.; Châtel, A., 2023. Assessment of microplastic contamination in the Loire River (France) throughout analysis of different biotic and abiotic freshwater matrices. Environmental Pollution, v. 334, 122167. https://doi.org/10.1016/j.envpol.2023.122167

Vithanage, M.; Prasad, M.N.V. (Eds.), 2023. Microplastics in the ecosphere: air, water, soil, and food. John Wiley & Sons, Hoboken.

Wang, C.; O'Connor, D.; Wang, L.; Wu, W.M.; Luo, J.; Hou, D., 2022. Microplastics in urban runoff: Global occurrence and fate. Water Research, v. 225, 119129. https://doi.org/10.1016/j.watres.2022.119129

Zhang, A.; Lipton, Z. C.; Li, M.; Smola, A.J., 2023. Dive into deep learning. Cambridge University Press, Cambridge.